The role of *CRP* and *ATG9B* expression in clear cell renal cell carcinoma

Running title: The role of *CRP* and *ATG9B* expression in CCRCC

Zheng Ma[1#], Zengguang Qi[2#], Jiangsong Li[1], Jing Yang[3], Zhonghua Xu[4*]

[1]Department of Urology, Liaocheng People's Hospital, Liaocheng, 252000, Shandong, China

[2]Department of Urology, Guanxian Center Hospital, Liaocheng, 252500, Shandong, China

[3]Department of Pediatrics, Liaocheng People's Hospital, Liaocheng, 252000, Shandong, China

[4]Department of Urology, Qilu Hospital of Shandong University, Jinan, 250012, Shandong, China

[#]**Zheng Ma and Zengguang Qi contributed equally to this work.**

[*]**Corresponding to: Zhonghua Xu,** Department of Urology, Qilu Hospital of Shandong University, No. 107, Cultural Western Road, Jinan, 250012, Shandong, China

Email: zhouxinjyk@163.com

Tel.: +86 053182166701

Funding: None

Abstract

Background: The purpose of the study is to investigate the correlation between the expression of C-reactive protein (*CRP*) and autophagy-related 9B (*ATG9B*) and pathological features of clear cell renal cell carcinoma (CCRCC) patients. We also intended to explore the effects of manipulated expression of *CRP* and *ATG9B* on the apoptosis and cell cycle progressing of CCRCC cell line.

Material and Methods: *ATG9B* expression in CCRCC tissues and adjacent renal tissues was analyzed by immunohistochemistry (IHC). Gene expression was determined at transcription and translational levels using real-time quantitative polymerase chain reaction (RT-qPCR) and western blot. The association between *CRP/ATG9B* expression and clinical-pathological parameters including age, gender, pathological grades, TNM stage and distant metastasis of the patients was assessed by correlation analysis. Small interfering RNA (siRNA) and overexpression plasmids construction were used to manipulate the expression of *CRP* in human CCRCC cell line 786-O. Cell apoptosis and cell cycle progressing were determined using flow cytometry and Hoechst 33258 staining.

Results: *CRP* expression correlates with *ATG9B* expression. The expression of *CRP* and *ATG9B* is significantly correlated with TNM staging, distant metastasis and survival time of CCRCC patients. A high-level of *CRP* indicates a poor overall survival (OS). In addition, *CRP* expression influences cell cycle and apoptosis of CCRCC cells.

Conclusion: The study reveals that *CRP* might be a CCRCC development promoter. In addition, there is a close relationship between *CRP* and *ATG9B* in CCRCC carcinogenesis.

Key words: clear cell renal cell carcinoma (CCRCC), *CRP*, *ATG9B*, cell apoptosis

Introduction

Renal cell carcinoma (RCC) is the most common substantial lesion within kidney (1), constituting 2%-3% of adult malignancies (2) and 85% of primary renal tumors (3). It commonly spreads to lungs, liver, bones, brain, adrenals, and lymph nodes, but seldom to skin, thyroid, and pancreas (4). Clear cell renal cell carcinoma (CCRCC), as a subtype of RCC, accounts for around 75% of RCC (5). 40 % of CCRCC patients would eventually die of carcinoma development (6). CCRCC shows the highest fatality rate among the common urologic malignancies (7). Over 10,000 patients die from kidney cancer each year, however, systemic treatment of RCC has been improved vastly in the last two decades (8). The pathogenesis of the most common type of RCC, CCRCC has been better understood. Therapies with high rates of response, longer progression-free survival such as anti-angiogenic drugs targeting vascular endothelial growth factor (VEGF) and its receptors and mechanistic target of rapamycin (mTOR) inhibitors have been used (9).

The C-reactive protein (*CRP*) is located on chromosome 1q23.2 and encodes protein that belongs to the pentaxin family. *CRP* is a plasma protein mainly generated in liver and activated by interleukin 6 (IL-6) (10). It is a prognostic factor for survival and recurrence of different types of cancers including mammary, prostatic, colonic, hepatocellular, bone and upper aerodigestive tract (UADT) tumors (11-14). Additionally, a previous meta-analysis has shown that high serum level of *CRP* (>1.0 mg/dl) is correlated with increased hazard of lung cancer and possibly breast, prostate and colorectal cancers (15). Furthermore, recent studies have revealed that *CRP* expression is significantly associated with overall survival (OS) time

of patients with RCC (16-19). However, whether abnormal *CRP* expression is associated with CCRCC pathogenesis, metastasis and OS remains to be clarified.

The autophagy-related 9B (*ATG-9B*), locating on chromosome 7q36.1, belongs to the *ATG* family. A previous study has shown that *ATG9B* expression is tissue-specific, that is, *ATG9B* is abundant in organs such as placenta and ovary but minimum in lung, testis, liver, muscle, brain and pancreas (20). The methylation of *ATG9B* promoter may interrupt the autophagy signal pathway and influence the invasive ductal carcinoma (IDC) development (21). Similarly, Kang *et al*. discovered that the mutation of *ATG9B* is common in human gastric and colorectal cancers and it can be closely related to stomach and colorectal carcinogenesis, suggesting that *ATG9B* mutation may promote neoplasm development by deregulating autophagy (22). What's more, *ATG9B* was found to be interacted with p38IP and regulated by p38α mitogen-activated protein kinase (MAPK) pathway, which then influenced the trafficking of *ATG9B* and therefore the autophagy process in a mammalian system (23, 24). Autophagy is closely related to cancer development including CCRCC (25, 26). However, the relationship between *ATG9B* expression and CCRCC pathogenesis, metastasis and OS remains to be clarified as well.

Previous studies have shown us the aberrant expression of *CRP* and *ATG9B* and their relationship with various human diseases especially cancer development including CCRCC. Yet, the influence of their expression on CCRCC progression remains further elaborated. Our study here aimed to explore the relationship between *CRP* and *ATG9B* expression with CCRCC pathogenesis, metastasis and survival as well as the role they play in CCRCC using

in vitro experiments.

Materials and Methods

Tissue specimens

185 CCRCC tissues and normal adjacent tissues were collected from CCRCC patients in the Urology Center of Liaocheng People's Hospital between 2013 and 2016. All tissues were frozen in liquid nitrogen immediately and were stored at -80□. No patients had received any adjuvant treatments, such as radiotherapy or chemotherapy before surgery. Written informed consents were obtained from all participants. The study had been approved by the Ethics Committee of Liaocheng People's Hospital.

Cell culture and siRNA transfection

CCRCC cell line (786-O) was purchased from American Type Culture Collection (ATCC; Manassas, VA, USA). All cells were placed in Dulbecco's Modified Eagle Medium (DMEM; Gibco, Life Technologies, Darmstadt, Germany) which contains 10% fetal bovine serum (FBS; HyClone, Logan, UT), penicillin (100 U/ml) and streptomycin (100 mg/ml). All were stored at 37□ in a humidified atmosphere containing 5% CO_2. SiRNA-1 and siRNA-2 were synthesized by Suzhou GenePharma Co., Ltd. (Suzhou, China). 24 h before transfection, the 786-O cells were seeded in the DMEM media with 10% FBS without antibiotics so the cells grew to 90% confluence. siRNA-Lipofectamine 2000 complexes were prepared. Briefly, siRNA-1 and siRNA-2 were resuspended in 1x siRNA buffer to reach a final concentration of 1 μM. 1 μl siRNA solution was added to 100 μl serum-free media to mix. 0.5 μl

Lipofectamine 2000 reagent was added to 25 μl serum-free media. siRNA media and diluted Lipofectamine 2000 reagent were incubated together for 20 min at room temperature to allow complex formation. The old media were removed after 4-6 h. The complexes were added to each well. Cells were then harvested 24 h after transfection. The siRNA sequences were provided in Table S1. SiRNA-1 and siRNA-2 were both used to knock down *CRP*, yet they had different sequences.

enzyme-linked immunosorbent assay (ELISA)

CRP Human ELISA Kit (ab99995, Abcam, Boston, MA, USA) was purchased for the conduction of ELISA. All materials were prepared at room temperature prior to use. 100 μl of standards and tissue samples were added to wells. The wells were covered ad incubated for 2.5 h. The solution was discarded and the wells were washed three times by adding 300 μl 1× wash solution into each well. Any remaining liquid was removed completely. 100 μl 1× biotinylated anti-human CRP detector antibody to each well. The antibody was incubated for 1 h. Then the solution was discarded and the wells were washed three times by adding 300 μl 1× wash solution into each well. 100 μl 1× HRP-Streptavidin solution to each well and incubated for 45 min. The solution was removed completely. 100 μl TMB One-Step substrate reagent was added to each well and incubated for 30 min in the dark. Lastly, 50 μl of Stop Solution was added to each well. The optimal density was read at 450 nm immediately.

RNA extraction and real-time quantitative polymerase chain reaction (RT-qPCR)

Total mRNAs of stored human CCRCC tissues and cells were extracted using Trizol reagent (Invitrogen, Carlsbad, CA, USA) following the manufacturer’s instructions. Reverse

transcribed complementary DNA (cDNA) synthesis was performed with PrimeScript RT reagent Kit (TaKaRa, Dalian, China). RT-qPCR was conducted using miSYBR-Green PCR kit (TransGen Biotech, China) according to manufacturer's protocols. Data were evaluated using SDS 2.2 software. GAPDH acted as the internal control. The expressions of *CRP* and *ATG9B* were quantified using $2^{-\Delta\Delta C_t}$ method. The primer sequence was listed in Table 1.

Immunohistochemical (IHC) staining

Three μm-thickness paraffin-embedded histotomy was soaked in xylene to dewax twice for 20 min, hydrated in gradient ethanol (100%, 90%, 80% and 70%) for 7 min. The specimens were then rinsed in the tap water three times, 3 min each time. The tissue sections were boiled with sodium citrate buffer for 5 min. The sections were then cultured in 3% H_2O_2 for 10 min to prevent endogenous peroxidase activities. The slices were then rinsed using phosphate-buffered saline (PBS) three times (5 min each time) and sealed in 10% serum for 10 min at room temperature to avoid non-specific binding. The tissue sections were subsequently incubated with primary antibodies anti-*CRP* antibody (ab31156, 5μg/ml, Abcam, Boston, MA, USA) and anti-*ATG9B* antibody (ab117591, 5 μg/ml, Abcam, Boston, MA, USA). After incubation at 4□ overnight with Galectin-3, the serum was discarded and the sections were mixed with biotinylated secondary antibodies for 10 min after being washed in PBS three times (5 min each time). Afterwards, the tissue sections were cultured with Streptavidin streptavidin-horseradish peroxidase (SA-HRP) for another 10 min and rinsed with PBS for 5 min, three times. Finally, after diluted with 3, 3' -diaminobenzidine (DAB), the sections were blended with Mayer's hematoxylin (Merck, Darmstadt, Germany), gradient

ethanol (95%, 85% and 75%) for 3 min respectively as well as absolute ethanol for 10 min and dehydrated in xylene twice, each time 5 min. The criteria IHC staining records were shown as follows: no expression (0 represents without staining), low expression (1 represents more than 30 % of cells weakly stained), or high expression (2 represents more than 30 % of cells strongly stained).

Western Blot

Cells were washed with PBS, scraped from the dishes and centrifuge at 12000 r.p.m., 4 °C for 15 min. Cell lysates were prepared with radioimmunoprecipitation assay (RIPA) buffer. The supernatants were collected and protein concentration was determined using the bicinchoninic acid BCA assay (Beyotime, Shanghai, China). Proteins were separated by sodium dodecyl sulfate–polyacrylamide gel electrophoresis (SDS-PAGE) (Bio-Rad, Hercules, CA, USA), transferred to a polyvinylidene difluoride (PVDF) membranes (Invitrogen, Gaithersburg, MD, USA) for western blot analysis following the manufacturer's guidelines. PVDF membranes were sealed using 5% skim milk for one hour at room temperature, and then incubated with primary antibodies anti-CRP (ab31156, 5μg/ml, Abcam, Boston, MA, USA) and Anti-ATG9B (ab117591, 2 μg/ml, Abcam, Boston, MA, USA). After cultured with primary antibodies overnight at 4℃, secondary antibodies (1:1000) were added for another one-hour incubation at room temperature. The membranes were washed three times with tris buffered saline-tween (TBST). The immunoreactive protein bands were visualized using G: Box XR5 and the membranes were subsequently exposed.

Hoechst 33258 staining

786-O cells were seeded on cover slips in 24-well plates. After transfection for 48 hours, cells were mixed with 4% paraformaldehyde at room temperature for 5 min. The cells were then permeabilized using 0.2 % Triton X-100 solution with PBS for another 5 min, and rinsed with PBS. Then 5 % BSA was used to block the cells at room temperature for 2 h, after which they were rinsed with PBS three times (5 min each time). The cells were then stained with 0.5 ml Hoechst 33258 in dark for 5 min and rinsed in PBS. Finally, they were coverslipped with aqueous mounting medium (Dako Faramount, Shanghai, China) for later observation.

Apoptosis assay

Flow cytometry (FCM) was employed to analyze the apoptosis of CCRCC cells. Cells were collected in logarithmic growth phase, placed in a 96-well plate and pre-incubated for 24h in a CO_2 incubator. Single-cell suspensions were fixed with 70 % alcohol and then rinsed twice with PBS and binding buffer was employed to re-suspend cells. For Annexin V staining, 5 μl Annexin V-PE, 5 μl 7-AAD staining and binding buffer of 10 mM 4-(2-hydroxyethyl)-1-piperazineethanesulfonic acid (HEPES)/ NaOH (pH 7.4), 140 mM NaCl, and 2.5 mM $CaCl_2$ were added to samples, which were incubated for 15 min at room temperature in dark and analyzed by a flow cytometer (FACSCanto II, BD Biosciences). The data were analyzed using FlowJo software (LLC, Ashland, OR, USA). Three experiments were performed in triplicate. Apoptotic cells that were positive of Annexin V-PE but not 7-AAD were early-apoptotic, whereas those were Annexin V-PE and 7-AAD positive were late-apoptotic or necrotic.

Statistical Analysis

SPSS 22 (Chicago, Illinois, USA) was used for statistical analyses and data were all presented as mean ± standard deviation (SD). Correlations between expressions of *CRP* and *ATG9B* and the clinic pathological characteristics were analyzed using two-sided Fisher's exact test. The correlation between the protein expressions of *CRP* and *ATG9B* was assessed using Spearman's rank correlation coefficient test. The Kaplan–Meier method was applied to draw overall survival (OS) curves and the expression comparisons distinction between groups was evaluated using the log-rank test. $P<0.05$ was considered statistically significant.

Results

The expression of *CRP* and *ATG9B* in serum and tissues

The concentration of CRP in human serum was evaluated using ELISA method. The results showed that the expression of CRP in CCRCC group was significantly higher than that in control group (<10 mg/L, Figure 1A). Meanwhile, among 185 CCRCC serum samples, there were high expressions of serum CRP in 159 cases (> 30 mg/L), moderate expression of CRP in 18 cases (11-30 mg/L) and lowly expression of CRP in 8 cases (< 10 mg/L).

The IHC staining results showed that compared with adjacent tissues, CCRCC tissues demonstrated more positive expression of ATG9B. In CCRCC tissues, low expression of ATG9B was detected in 82 patients and highly expressed ATG9B was observed in 103 patients (Figure 1B). The positive signal was in the cytoplasm of cancer cells.

The correlation between gene expression and the pathological characteristics of CCRCC patients

The relationship between *CRP* and *ATG9B* expression levels and CCRCC patients' characteristics were analyzed using two-sided Fisher's exact test. As was shown in Table 2, high expression of *CRP* or *ATG9B* was positively related to advanced TNM stage and distant metastases. In addition, there was also a positive correlation between *CRP* expression and *ATG9B* expression (Table 3).

The correlation between *CRP* expression and patients' prognosis

Survival curves were generated by means of the Kaplan–Meier method and the distinctions among groups with different expressions were detected using the log-rank test. The correlation between *CRP* expression level and overall survival (OS) of CCRCC patients was shown in Figure 1C. The results indicated that patients with high *CRP* expression level had a lower OS and poorer prognostic result than those who with low *CRP* expression level.

The correlation between *CRP* expression and *ATG9B* expression

The effect of small interfering RNA (siRNA) transfection on the expression of *CRP* was confirmed by RT-qPCR (Figure 2A). Compared with the negative control group, siRNAs (siRNA-1 and siRNA-2) could significantly inhibit *CRP* mRNA expression. *ATG9B* expression dramatically decreased after the transfection of siRNAs. In addition, the expression level of *ATG9B* decreased more quickly than that of *CRP* (Figure 2B). According to western blot results, the expression levels of *CRP* and *ATG9B* proteins were remarkably downregulated.

The inhibitive effects of *CRP* on the apoptosis of 786-O cells

The results of Hoechst 33258 staining of the tumor cell cytoplasm showed that the

transfection of siRNAs significantly promoted the apoptosis of 786-O cells (Figure 3A). Annexin-V and 7-AAD dual-staining flow cytometry results demonstrated that the apoptosis rate of cells in siRNA-1 or siRNA-2 group was much higher than that in the control group (Figure 3B). This also indicated that the apoptosis of 786-O cells could be induced through silencing *CRP* expression. On the other hand, cell cycle assay also demonstrated that cells were arrested in G1 phase in the two siRNA groups (Figure 3C).

The synchronous expression of *CRP* expression and *ATG9B* expression

As shown in Figure 4, mRNA expression levels of *CRP* and *ATG9B* in overexpressed group was upregulated by more than twice in comparison with the control group. Western blot results revealed that overexpression of *CRP* could significantly up-regulate the expression of *ATG9B.*

The inhibitive effects of *CRP* expression on the apoptosis in 786-O cells

The apoptotic rate of the overexpression group presented a drastic decline in comparison with negative control group, which also suggested *CRP* overexpression could inhibit apoptosis (Figure 5A). Moreover, *CRP* expression group displayed much fewer apoptotic cells than the negative control group, shown by Annexin-V and 7-AAD dual-staining flow cytometry test results. *CRP* overexpression could suppress cell apoptosis (Figure 5B). S and G2/M phases increased in 786-O cells of overexpression group compared to the negative control group (Figure 5C). This showed that *CRP* expression level could exert influence on the cell cycle of 786-O cells.

Discussion

In this study, we have discovered that the expression of *CRP* and *ATG9B* is significantly correlated with CCRCC TNM staging, metastasis and OS. A higher level of *CRP* indicates a poorer OS of CCRCC patient. The inhibition of *CRP* expression significantly increased the apoptosis and cell cycle arrest of CCRCC cell line 786-O. *CRP* expression is positively correlated with *ATG9B*, and its overexpression led to less apoptosis and less cell cycle arrest of 786-O cells. CCRCC is the most common kind of RCC with poor prognosis with 5-year survival rate of 0%~10% (27). To understand the relationship of *CRP* and *ATG9B* expression and CCRCC is significant to the development of CCRCC prognosis and treatment.

In our study, we found that *CRP* expression was associated with *ATG9B* expression. The inhibition of *CRP* expression was accompanied by decreased expression of *ATG9B* and the overexpression of *CRP* was accompanied with increased expression of *ATG9B*. Serum *CRP* protein was low-expressed in normal patients. Among CCRCC patients, 159 were found with high-level *CRP* (> 30 mg/L), 18 medium-level (11-30 mg/L) and 8 low-level (< 10 mg/L). On the other hand, *ATG9B* was found overexpressed in most of CCRCC patients. *CRP* was found significantly associated with OS of CCRCC patients. Based on the above results, we speculated that the expression of *CRP* and *ATG9B* was positively correlated with CCRCC and it may indicate a poorer status of CCRCC. Our results are consistent with previous studies, in which identical findings were demonstrated in regards of RCC OS and aberrant *CRP* expression (17, 28-30). Thus, we speculated that the aberrant overexpression of *CRP* and *ATG9B* could possibly promote CCRCC development.

The *in vivo* experiment results support our hypothesis that the aberrant overexpression of *CRP* and *ATG9B* could promote CCRCC development, possibly by influencing the cell cycle and apoptosis. The inhibition of *CRP* expression promoted whereas the promotion of *CRP* expression inhibited 786-O cell cycle arrest and apoptosis. As a stable downstream inflammation marker, it can be stimulated by IL-1 and tumor necrosis factors (TNFs) (31). Chronic inflammation can be predictor of cancer initiation, progression, metastasis and survival. *CRP*-level measurements can be clinically significant for RCC prognosis (32, 33). Hence, we inferred that *CRP* could be involved in CCRCC development via some inflammation pathway that involves ILs and TNFs and affect CCRCC cell proliferation and apoptosis.

On the other hand, *CRP* overexpression was found accompanied/associated with *ATG9B* overexpression. *ATG9B* is involved in autophagy process that delivers cytoplasmic constituents degraded by autophagosomes to lysosomes for digestion (34), which is a common scene during carcinogenesis (26). Autophagy can play a protective role in tumor cell survival, and can also contribute to cancer progression by preventing tumor cell from programing death (35). Zhang *et al.* found aberrant promoter methylation of *ATG9B* in sporadic breast carcinoma (21). Oncogenic autophagy in clear cell renal cell carcinoma was reported to be regulated by some molecules, which could contribute to the CCRCC progression (25). *ATG* genes as well as ATG-interacted genes have been reported to be related to the development of diverse carcinomas such as lung cancer and CCRCC *etc.* (36). Based on the previous findings as well as ours, we speculated that aberrant *ATG9B* expression might

contribute to the aberrant autophagy of CCRCC cells, which then induced CCRCC progression.

Certain limitations exist in this study. First of all, *in vivo* studies need to be done to elaborate the role of *CRP* and *ATG9B* expression during CCRCC development. Secondly, *ATG9B*-related autophagy pathway can be further studied for a better comprehension of the *ATG9B*-related mechanism of CCRCC pathogenesis. Thirdly, the influence between *CRP*-related inflammation pathways and CCRCC need to be further explored. Fourthly, *in vivo* experiments need to be further studied to verify the *in vitro* discoveries. Lastly, detailed correlation between *ATG9B* and CCRCC pathogenesis need further investigation as well.

In conclusion, our study showed that *CRP* and *ATG9B* were both aberrantly overexpressed in CCRCC tissues and cells, and they were closely correlated with CCRCC TNM staging, metastasis and OS. The suppression of *CRP* expression led to the cancer cell cycle arrest and apoptosis. The results indicate that *CRP* and *ATG9B* could be significant predictors of CCRCC and can be a valuable target for CCRCC therapy.

Declarations

Ethics approval and consent to participate: All procedures of this research were in accordance with the Declaration of Helsinki and approved by the Ethics Committee of Liaocheng People's Hospital. All patients participated have given consent to this study.

Conflicts of interest: All authors declare that they have no conflict of interest.

Acknowledgements: Not applicable.

Author contributions: Research conception and design: Zheng Ma and Zengguang Qi; Data analysis and interpretation: Jiangsong Li and Jing Yang; Drafting of the manuscript: Zheng Ma and Zengguang Qi; Critical revision of the manuscript: Zhonghua Xu; Approval of final manuscript: all authors.

References

1. Ozturk H. Bilateral synchronous adrenal metastases of renal cell carcinoma: A case report and review of the literature. Oncol Lett. 2015;9(4):1897-901.

2. Flum AS, Hamoui N, Said MA, Yang XJ, Casalino DD, McGuire BB, et al. Update on the Diagnosis and Management of Renal Angiomyolipoma. J Urol. 2016;195(4 Pt 1):834-46.

3. Bokhari A, Tiscornia-Wasserman PG. Cytology diagnosis of metastatic clear cell renal cell carcinoma, synchronous to pancreas, and metachronous to thyroid and contralateral adrenal: Report of a case and literature review. Diagn Cytopathol. 2017;45(2):161-7.

4. Wolf S, Obolonczyk L, Sworczak K, Czapiewski P, Sledzinski Z. Renal cell carcinoma metastases to the pancreas and the thyroid gland 19 years after the primary tumour. Prz Gastroenterol. 2015;10(3):185-9.

5. Feng C, Xiong Z, Jiang H, Ding Q, Fang Z, Hui W. Genetic alteration in notch pathway is associated with better prognosis in renal cell carcinoma. Biofactors. 2016;42(1):41-8.

6. Wendel C, Campitiello M, Plastino F, Eid N, Hennequin L, Quetin P, et al. Pituitary Metastasis from Renal Cell Carcinoma: Description of a Case Report. Am J Case Rep. 2017;18(7-11.

7. Xu ZQ, Zhang L, Gao BS, Wan YG, Zhang XH, Chen B, et al. EZH2 promotes tumor progression by increasing VEGF expression in clear cell renal cell carcinoma. Clin Transl Oncol. 2015;17(1):41-9.

8. Ouyang AM, Wei ZL, Su XY, Li K, Zhao D, Yu DX, et al. Relative Computed Tomography (CT) Enhancement Value for the Assessment of Microvascular Architecture in Renal Cell

Carcinoma. Med Sci Monit. 2017;23(3706-14.

9. Choueiri TK, Motzer RJ. Systemic Therapy for Metastatic Renal-Cell Carcinoma. N Engl J Med. 2017;376(4):354-66.

10. Bereta J, Kurdowska A, Koj A, Hirano T, Kishimoto T, Content J, et al. Different preparations of natural and recombinant human interleukin-6 (IFN-beta 2, BSF-2) similarly stimulate acute phase protein synthesis and uptake of alpha-aminoisobutyric acid by cultured rat hepatocytes. Int J Biochem. 1989;21(4):361-6.

11. Nakamura T, Grimer RJ, Gaston CL, Watanuki M, Sudo A, Jeys L. The prognostic value of the serum level of C-reactive protein for the survival of patients with a primary sarcoma of bone. Bone Joint J. 2013;95-B(3):411-8.

12. Nakamura T, Grimer R, Gaston C, Francis M, Charman J, Graunt P, et al. The value of C-reactive protein and comorbidity in predicting survival of patients with high grade soft tissue sarcoma. Eur J Cancer. 2013;49(2):377-85.

13. Funovics PT, Edelhauser G, Funovics MA, Laux C, Berzaczy D, Kubista B, et al. Pre-operative serum C-reactive protein as independent prognostic factor for survival but not infection in patients with high-grade osteosarcoma. Int Orthop. 2011;35(10):1529-36.

14. Nakanishi H, Araki N, Kudawara I, Kuratsu S, Matsumine A, Mano M, et al. Clinical implications of serum C-reactive protein levels in malignant fibrous histiocytoma. Int J Cancer. 2002;99(2):167-70.

15. Guo YZ, Pan L, Du CJ, Ren DQ, Xie XM. Association between C-reactive protein and risk of cancer: a meta-analysis of prospective cohort studies. Asian Pac J Cancer Prev.

2013;14(1):243-8.

16. Guo S, He X, Chen Q, Yang G, Yao K, Dong P, et al. The C-reactive protein/albumin ratio, a validated prognostic score, predicts outcome of surgical renal cell carcinoma patients. BMC Cancer. 2017;17(1):171.

17. Dalpiaz O, Luef T, Seles M, Stotz M, Stojakovic T, Pummer K, et al. Critical evaluation of the potential prognostic value of the pretreatment-derived neutrophil-lymphocyte ratio under consideration of C-reactive protein levels in clear cell renal cell carcinoma. Br J Cancer. 2017;116(1):85-90.

18. Fujita T, Nishi M, Tabata K, Matsumoto K, Yoshida K, Iwamura M. Overall prognostic impact of C-reactive protein level in patients with metastatic renal cell carcinoma treated with sorafenib. Anticancer Drugs. 2016;27(10):1028-32.

19. Hu H, Yao X, Xie X, Wu X, Zheng C, Xia W, et al. Prognostic value of preoperative NLR, dNLR, PLR and CRP in surgical renal cell carcinoma patients. World J Urol. 2017;35(2):261-70.

20. Kusama Y, Sato K, Kimura N, Mitamura J, Ohdaira H, Yoshida K. Comprehensive analysis of expression pattern and promoter regulation of human autophagy-related genes. Apoptosis. 2009;14(10):1165-75.

21. Zhang X, Li C, Wang D, Chen Q, Li CL, Li HJ. Aberrant methylation of ATG2B, ATG4D, ATG9A and ATG9B CpG island promoter is associated with decreased mRNA expression in sporadic breast carcinoma. Gene. 2016;590(2):285-92.

22. Kang MR, Kim MS, Oh JE, Kim YR, Song SY, Kim SS, et al. Frameshift mutations of

autophagy-related genes ATG2B, ATG5, ATG9B and ATG12 in gastric and colorectal cancers with microsatellite instability. J Pathol. 2009;217(5):702-6.

23. Webber JL, Tooze SA. New insights into the function of Atg9. FEBS Lett. 2010;584(7):1319-26.

24. Webber JL, Tooze SA. Coordinated regulation of autophagy by p38alpha MAPK through mAtg9 and p38IP. EMBO J. 2010;29(1):27-40.

25. Hall DP, Cost NG, Hegde S, Kellner E, Mikhaylova O, Stratton Y, et al. TRPM3 and miR-204 establish a regulatory circuit that controls oncogenic autophagy in clear cell renal cell carcinoma. Cancer Cell. 2014;26(5):738-53.

26. Cecconi F, Jaattela M. Targeting ions-induced autophagy in cancer. Cancer Cell. 2014;26(5):599-600.

27. Zeng FC, Zeng MQ, Huang L, Li YL, Gao BM, Chen JJ, et al. Downregulation of VEGFA inhibits proliferation, promotes apoptosis, and suppresses migration and invasion of renal clear cell carcinoma. Onco Targets Ther. 2016;9(2131-41.

28. Kuang H, Liao L, Chen H, Kang Q, Shu X, Wang Y. Therapeutic Effect of Sodium Glucose Co-Transporter 2 Inhibitor Dapagliflozin on Renal Cell Carcinoma. Med Sci Monit. 2017;23(3737-45.

29. Novara G. Editorial comment on: Impact of C-reactive protein kinetics on survival of patients with metastatic renal cell carcinoma. Eur Urol. 2009;55(5):1153-4.

30. Yoshida N, Ikemoto S, Narita K, Sugimura K, Wada S, Yasumoto R, et al. Interleukin-6, tumour necrosis factor alpha and interleukin-1beta in patients with renal cell carcinoma. Br J

Cancer. 2002;86(9):1396-400.

31. Hu Q, Gou Y, Sun C, Ding W, Xu K, Gu B, et al. The prognostic value of C-reactive protein in renal cell carcinoma: a systematic review and meta-analysis. Urol Oncol. 2014;32(1):50 e1-8.

32. Shrotriya S, Walsh D, Bennani-Baiti N, Thomas S, Lorton C. C-Reactive Protein Is an Important Biomarker for Prognosis Tumor Recurrence and Treatment Response in Adult Solid Tumors: A Systematic Review. PLoS One. 2015;10(12):e0143080.

33. Hrab M, Olek-Hrab K, Antczak A, Kwias Z, Milecki T. Interleukin-6 (IL-6) and C-reactive protein (CRP) concentration prior to total nephrectomy are prognostic factors in localized renal cell carcinoma (RCC). Rep Pract Oncol Radiother. 2013;18(5):304-9.

34. Zavodszky E, Vicinanza M, Rubinsztein DC. Biology and trafficking of ATG9 and ATG16L1, two proteins that regulate autophagosome formation. FEBS Lett. 2013;587(13):1988-96.

35. Mizushima N, Levine B, Cuervo AM, Klionsky DJ. Autophagy fights disease through cellular self-digestion. Nature. 2008;451(7182):1069-75.

36. Lebovitz CB, Robertson AG, Goya R, Jones SJ, Morin RD, Marra MA, et al. Cross-cancer profiling of molecular alterations within the human autophagy interaction network. Autophagy. 2015;11(9):1668-87.

Figure Legends

Figure 1 *CRP* and *ATG9B* expression in tissues and the relationship between *CRP* expression and overall survival rate of patients. A: Serum *CRP* protein was low-expressed in patients of the normal group, but high-expressed (> 30 mg/L) in 159 CCRCC cases, medium-expressed in 18 CCRCC cases (11-30 mg/L) and low-expressed (< 10 mg/L) in 8 CCRCC cases. **B:** *ATG9B* expression in all normal kidney and tumorous tissues was positive, with 82 low-expressed and 103 high-expressed in CCRCC patients group. The positive signal is in the cancer cell cytoplasm. **C:** Patients with high *CRP* expression level had worse survival outcomes compared to low expression group. * $P<0.05$ compared to control group.

Figure 2 *CRP* silences effects and its correlation with *ATG9B* expression A: siRNAs could significantly down-regulate mRNA expressions of *CRP* and *ATG9B* protein. mRNA levels of *CRP* and *ATG9B* were both significantly lower in siRNA-1 and siRNA-2 groups than in control group. **B:** *CRP* protein level as well as *ATG9B* protein level in siRNA-1 and siRNA-2 groups was much lower than in control group. *$P<0.05$, # $P<0.05$ compared to control group.

Figure 3 Inhibition of *CRP* expression induces cell cycle arrest and the apoptosis of 786-O cells A: The apoptosis of 786-O cells increased by either siRNA by approximately 2.5 times. Scale bar: 30 μm. **B:** Dual-staining flow cytometry test results showed that apoptotic cells transfected with siRNAs were much more than those in the control group. * means $P<0.05$ compared to the control group. **C:** The cell cycle was significantly arrested in G0/G1 phase in siRNA groups. * $P<0.05$ compared to control group.

Figure 4 The effects of *CRP* overexpression and its correlation with *ATG9B* expression A:

CRP mRNA expression increased by approximately 2.5 times, while *ATG9B* expression increased by approximately 2.2 times significantly in *CRP* overexpression group than in Scr group. **B:** CRP level increased significantly because of its overexpression, which also improved ATG9B level. * $P<0.05$, # $P<0.05$ compared to Scr group.

Figure 5 *CRP* overexpression promotes the apoptosis of 786-O cells and reduces the cell cycle A: 786-O cell apoptosis decreased by approximately two-fold. Scale bar: 30 μm**. B:** the number of apoptotic cells was much less in CRP overexpression group than that in Scr group. **C:** The percentage of cells that were arrested in G0/G1 phase in CRP overexpression group was reduced significantly compared to Scr group. * $P<0.05$ compared to Scr group.

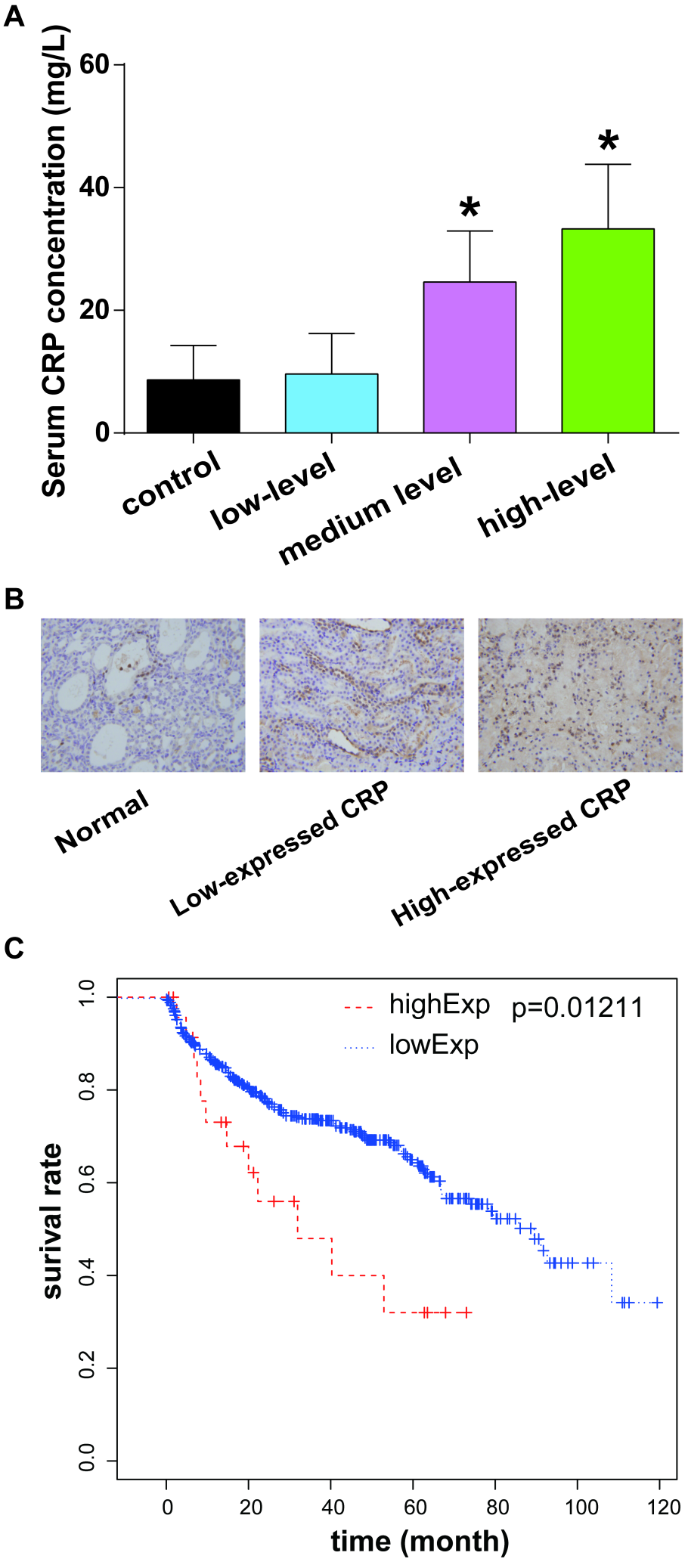
A
Serum CRP concentration (mg/L)
60
40
20
0
*
*
control
low-level
medium level
high-level
B
Normal
Low-expressed CRP
High-expressed CRP
C
surival rate
1.0
0.8
0.6
0.4
0.2
0.0
highExp p=0.01211
lowExp
0
20
40
60
80
100
120
time (month)

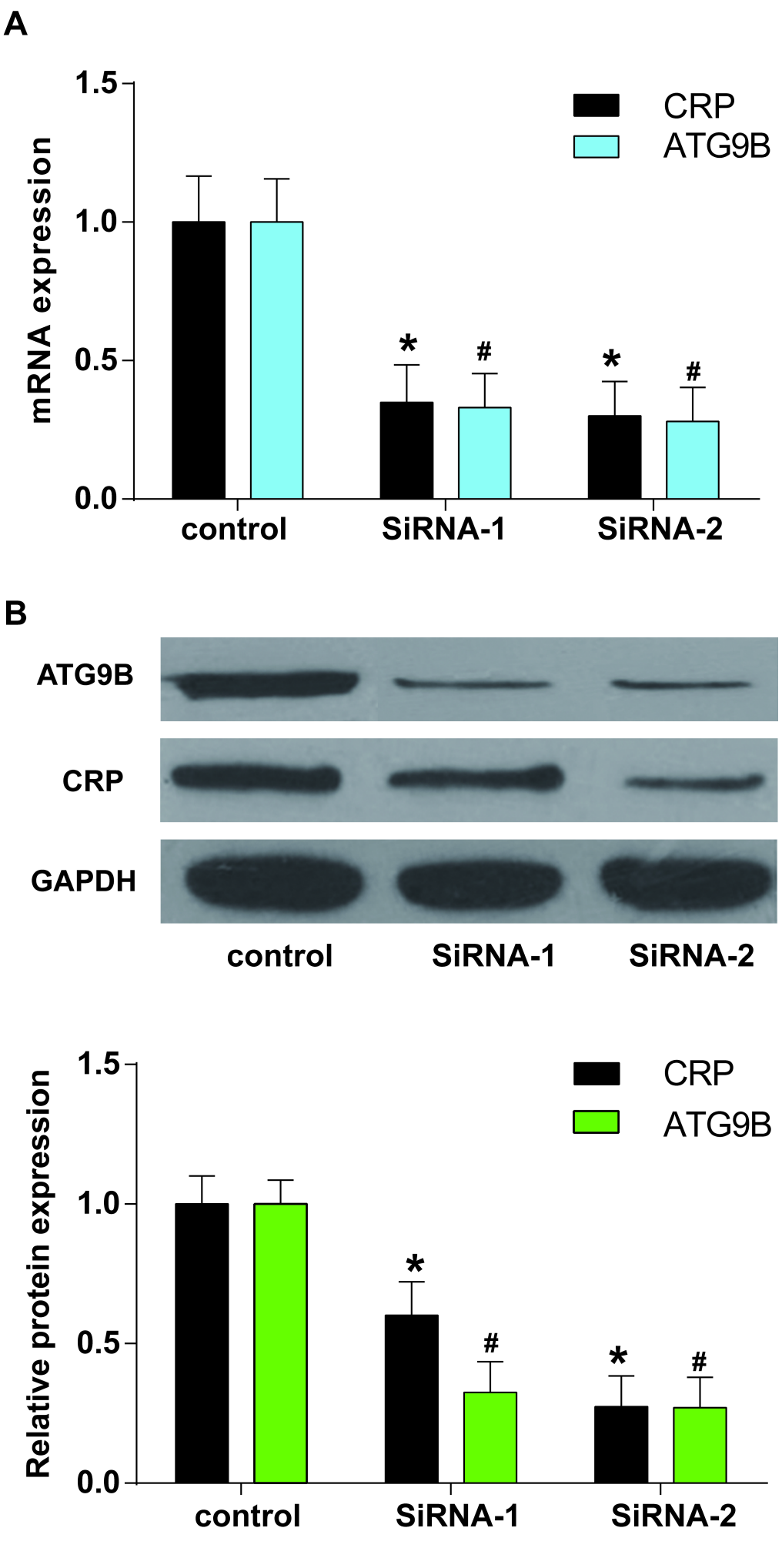
A
1.5
1.0
0.5
0.0
mRNA expression
CRP
ATG9B
*
#
*
#
control
SiRNA-1
SiRNA-2
B
ATG9B
CRP
GAPDH
control
SiRNA-1
SiRNA-2
1.5
1.0
0.5
0.0
Relative protein expression
CRP
ATG9B
*
#
*
#
control
SiRNA-1
SiRNA-2

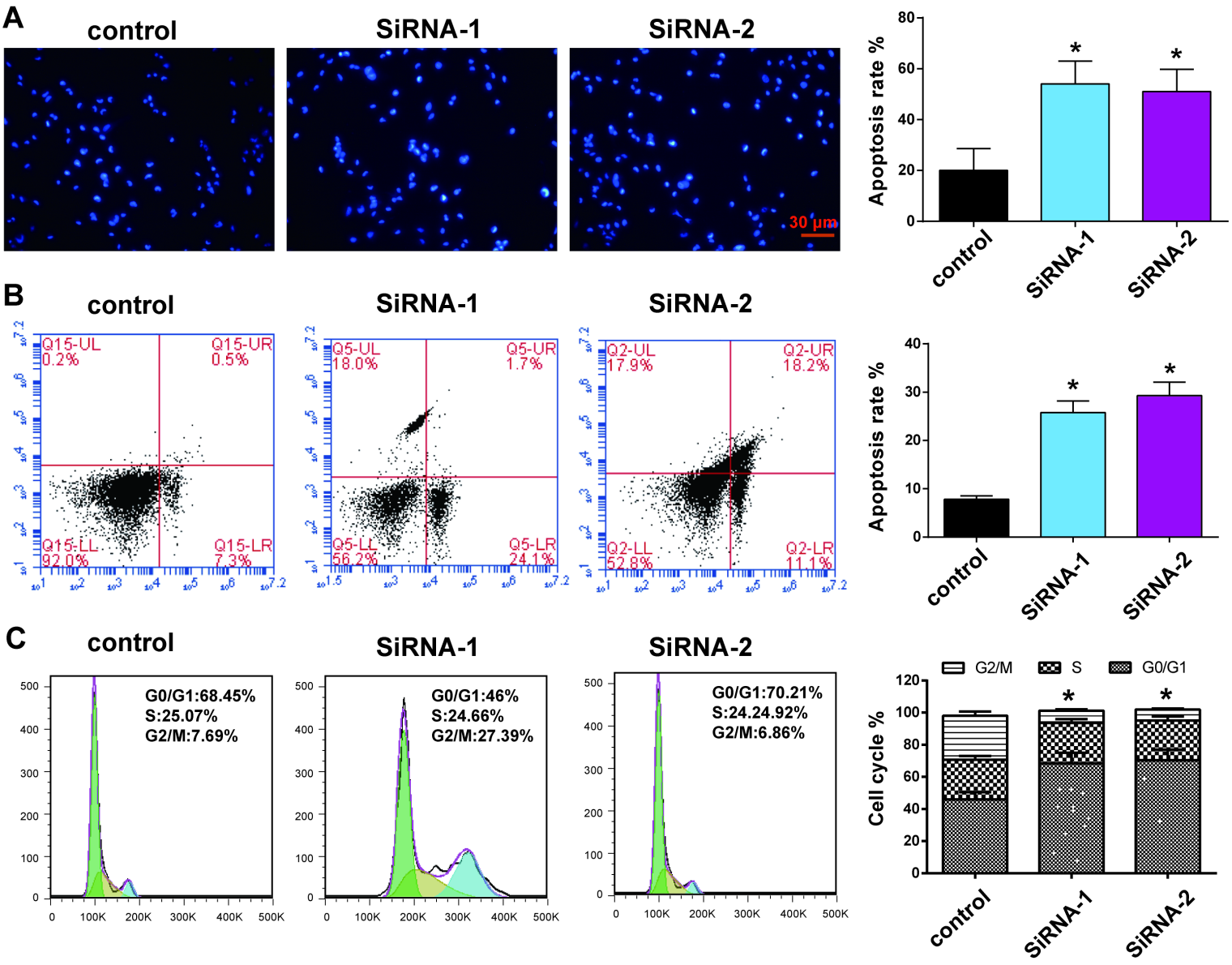
A
control
SiRNA-1
SiRNA-2
30 μm
Apoptosis rate %
80
60
40
20
0
*
*
control
SiRNA-1
SiRNA-2
B
control
SiRNA-1
SiRNA-2
Q15-UL
0.2%
Q15-UR
0.5%
Q15-LL
92.0%
Q15-LR
7.3%
Q5-UL
18.0%
Q5-UR
1.7%
Q5-LL
56.2%
Q5-LR
24.1%
Q2-UL
17.9%
Q2-UR
18.2%
Q2-LL
52.8%
Q2-LR
11.1%
Apoptosis rate %
40
30
20
10
0
*
*
control
SiRNA-1
SiRNA-2
C
control
SiRNA-1
SiRNA-2
G0/G1:68.45%
S:25.07%
G2/M:7.69%
G0/G1:46%
S:24.66%
G2/M:27.39%
G0/G1:70.21%
S:24.24.92%
G2/M:6.86%
500
400
300
200
100
0
0
100K
200K
300K
400K
500K
G2/M
S
G0/G1
Cell cycle %
120
100
80
60
40
20
0
*
*
control
SiRNA-1
SiRNA-2

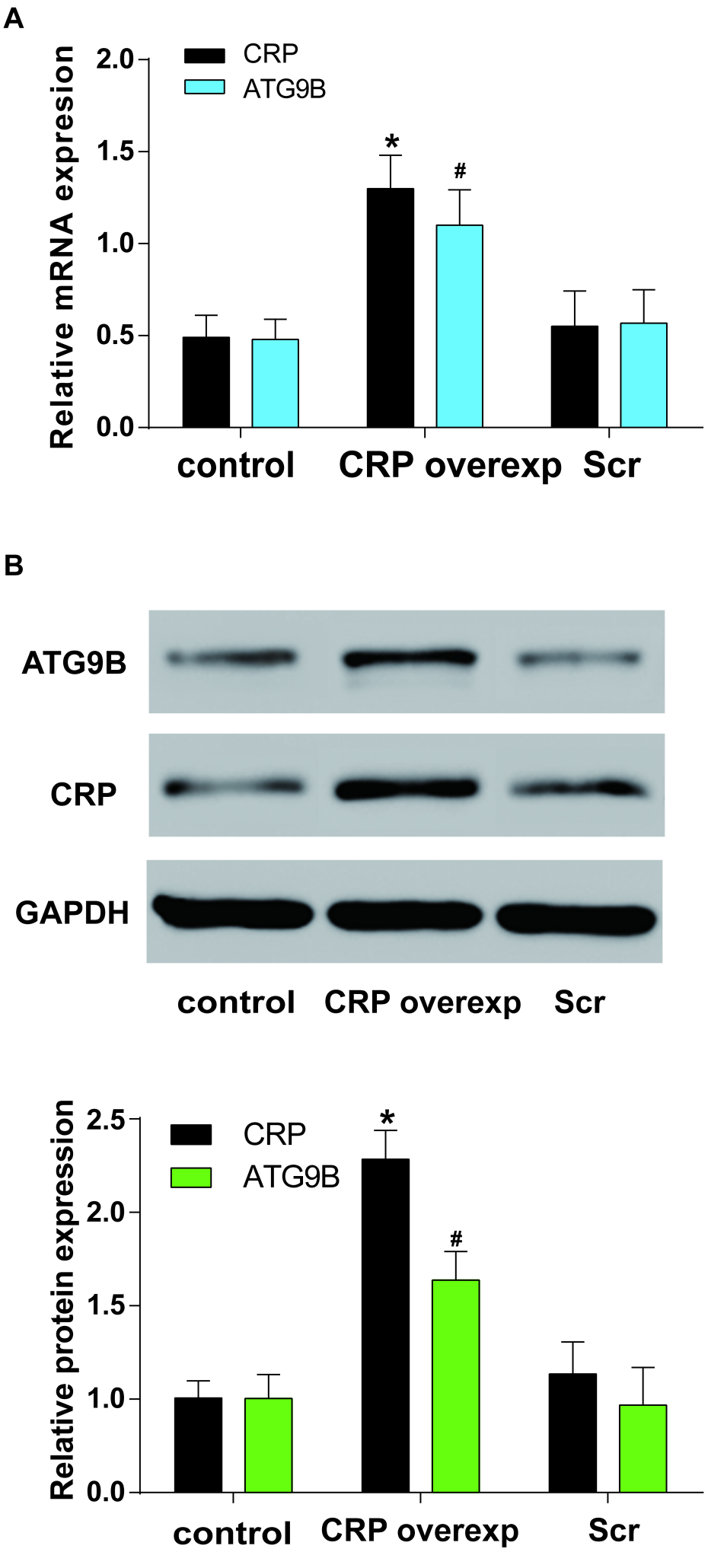
A
CRP
ATG9B
Relative mRNA expresion
2.0
1.5
1.0
0.5
0.0
*
#
control
CRP overexp
Scr
B
ATG9B
CRP
GAPDH
control
CRP overexp
Scr
CRP
ATG9B
Relative protein expression
2.5
2.0
1.5
1.0
0.0
*
#
control
CRP overexp
Scr

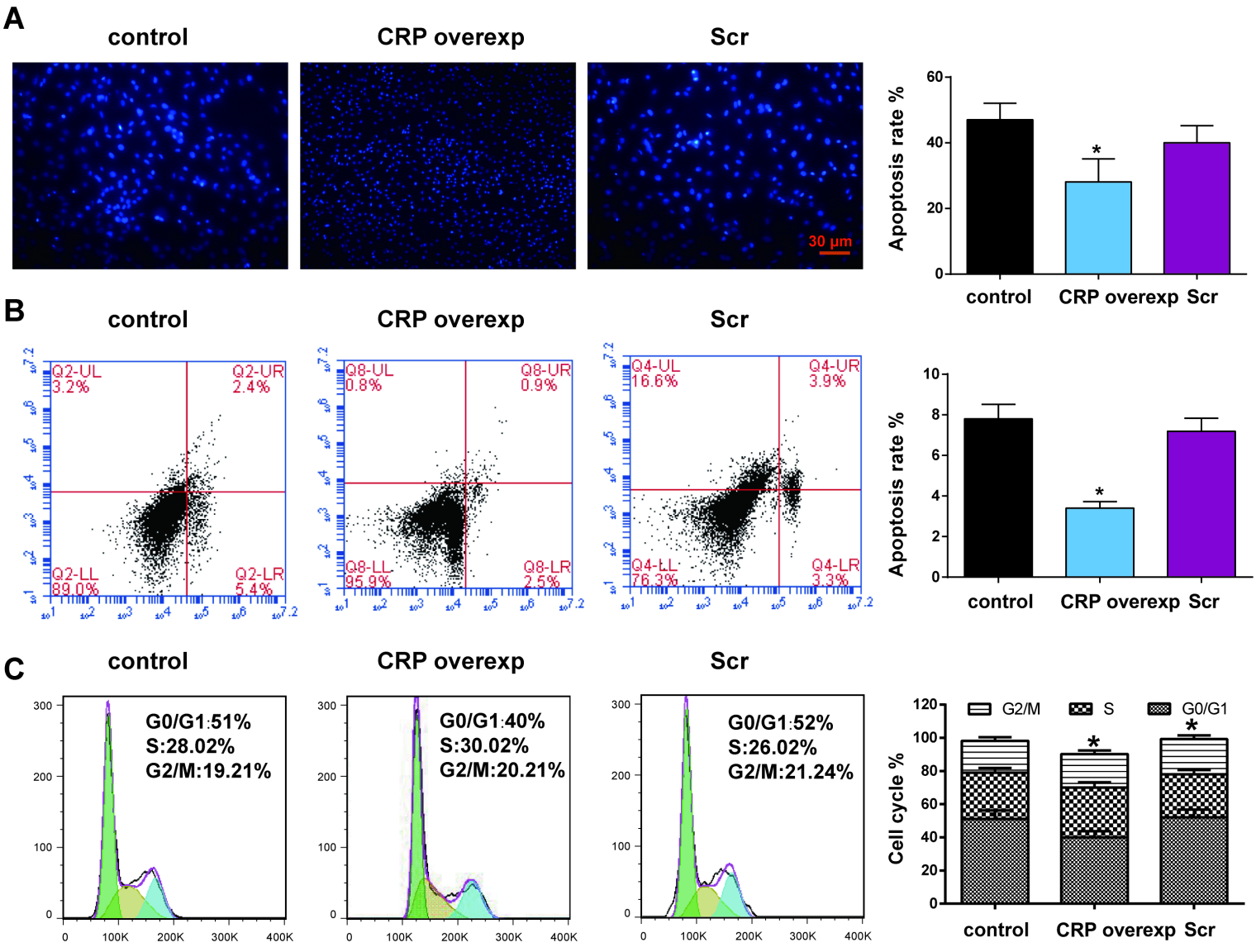
A
control
CRP overexp
Scr
30 μm
Apoptosis rate %
60
40
20
0
*
control
CRP overexp
Scr
B
control
CRP overexp
Scr
Q2-UL
3.2%
Q2-UR
2.4%
Q2-LL
89.0%
Q2-LR
5.4%
Q8-UL
0.8%
Q8-UR
0.9%
Q8-LL
95.9%
Q8-LR
2.5%
Q4-UL
16.6%
Q4-UR
3.9%
Q4-LL
76.3%
Q4-LR
3.3%
Apoptosis rate %
10
8
6
4
2
0
*
control
CRP overexp
Scr
C
control
CRP overexp
Scr
G0/G1:51%
S:28.02%
G2/M:19.21%
G0/G1:40%
S:30.02%
G2/M:20.21%
G0/G1:52%
S:26.02%
G2/M:21.24%
300
200
100
0
0
100K
200K
300K
400K
Cell cycle %
120
100
80
60
40
20
0
G2/M
S
G0/G1
*
*
control
CRP overexp
Scr

Table 1 RT-qPCR Primer Sequences

Gene name	Primers (5’-3’)
CRP	F: TGTGAGCCAGAAAAACAAGCAAA
	R: GGTATGGGGGTGGGGTCTAA
ATG9B	F: TGTGAGCCAGAAAAACAAGCAAA
	R: GGTATGGGGGTGGGGTCTAA
GAPDH	F: TGTGAGCCAGAAAAACAAGCAAA
	R: GGTATGGGGGTGGGGTCTAA

Table 2 Associations between expressions of CRP and ATG9B and clinicopathologic characteristics in clear cell RCC patients

Characteristics	Volume (%)	CRP expression (*N* = 185)		*p*	ATG9B expression (*N* = 185)		*p*
		Low (*N*=97) (%)	High (*N*=88) (%)		Low (*N*=82) (%)	High (*N*=88) (%)	
Age (years)							
≤52	73 (39.46)	36 (49)	37 (51)	0.548	38 (52)	35 (48)	0.097
>52	112 (60.54)	61 (55)	51 (45)		44 (39)	68 (61)	
Gender							
Male	105 (56.76)	52 (49)	53 (51)	0.377	51 (49)	54 (51)	0.232
Female	80 (43.24)	45 (56)	35 (44)		31 (39)	49 (61)	
Histologic Grade							
Grade 1-2	77 (41.62)	39 (51)	38 (49)	0.765	37 (48)	40 (52)	0.453
Grade 3-4	108 (58.38)	58 (54)	50 (46)		45 (42)	63 (58)	
TNM stage							
I-II	98 (52.97)	60 (61)	38 (39)	**0.013**	32 (33)	66 (67)	**0.001**
III-IV	87 (47.03)	37 (43)	50 (57)		50 (57)	37 (43)	
Distant metastasis							
Absent	127 (68.65)	75 (59)	52 (41)	**0.011**	63 (49)	64 (51)	**0.038**
Present	58 (31.35)	22 (38)	36 (62)		19 (33)	39 (67)	

Table 3 Correlations between CRP and ATG9B

Spearman's rho		CRP	ATG9B
CRP	Correlation Coefficient	1.000	0.850
	Sig.（2-tailed）	0.000	0.000
ATG9B	Correlation Coefficient	0.850	1.000
	Sig.（2-tailed）	0.000	0.000

Table S1 SiRNA sequences that were used in the experiments.

	Site	DNA sequence		
siRNA-1	1482-1504	GCGCTGATCTTCTATTTAA	Sense 5’-3’	GCGCUGAUCUUCUAUUUAA
			Antisense 3’-5’	CGCGACUAGAAGAUAAAUU
siRNA-2	705-727	GTGGGTGGGTCTGAAATAT	Sense 5’-3’	GUGGGUGGGUCUGAAAUAU
			Antisense 3’-5’	CACCCACCCAGACUUUAUA